ELSEVIER

International Journal of Pharmaceutics 153 (1997) 147–157

international journal of pharmaceutics

Evaluation of the anticancer action of a permanently charged tamoxifen derivative, tamoxifen methiodide: an MRI study

Marcus E. Brewster [a,b,c], Yael Paran [b], Edna Rushkin [b], Anat Biegon [c], Emil Pop [a], Hadassa Degani [b,*]

[a] *Pharmos Corporation, Two Innovation Drive, Alachua, FL 32615, USA*
[b] *Department of Biological Regulation, Weizmann Institute of Science, Rehovot 76100, Israel*
[c] *Pharmos Limited, Kiryat Weizmann, Rehovot 76326, Israel*

Received 2 December 1996; received in revised form 12 February 1997; accepted 13 February 1997

Abstract

The anticancer action of a permanently charged tamoxifen derivative, tamoxifen methiodide (TMI), was assessed in a model of breast cancer. In addition, analysis of MCF-7 cells in cultures was performed to consider the anticancer mechanism of TMI. Nude mice were implanted with MCF-7 human cancer cells in the ventral fat pad at the level of the milkline (breast). The effect of TMI (administered as a slow-release pellet) and placebo were evaluated using magnetic resonance imaging (MRI) as well as by histological evaluation. The action of TMI and tamoxifen on cell growth of MCF-7 cells in cultures was also assessed. TMI induced tumor regression, while placebo-treated animals manifested tumor masses that grew monotonically throughout the experimental period (25 days). MRI revealed and histopathology confirmed that TMI treatment resulted in tumor necrosis which (1) had a faster onset; (2) was more extensive; and (3) was more intense than that observed by partial estrogen ablation (placebo-treated animals). Studies with MCF-7 cells in culture suggested that tamoxifen and TMI are equipotent in vitro. Given various reports that TMI is more potent than tamoxifen in vivo and that the anticancer efficacy between TMI and tamoxifen cannot be explained by differences in estrogen receptor interaction or effects on MCF-7S cell in culture, other mechanism may differentially contribute to the anticancer action of TMI. © 1997 Elsevier Science B.V.

Keywords: Tamoxifen methiodide (TMI); Tamoxifen; Breast cancer; MCF-7 cell culture; Magnetic resonance imaging (MRI)

* Corresponding author.

0378-5173/97/$17.00 © 1997 Elsevier Science B.V. All rights reserved.
PII S0378-5173(97)04921-1

1. Introduction

Breast cancer is the single most common malignancy in women in the US and, after lung cancer, the leading cause of cancer-related deaths. In 1993, it was estimated that 183 000 women developed breast cancer of whom 46 000 died of the disease (Love, 1991; Grady et al., 1992; Telang et al., 1992; Wong et al., 1992; Love and Koroltchouk, 1993; El-Ashry and Lippman, 1994). Meta-analysis of clinical and epidemiological studies published since 1970 indicate that a 50 year old woman has a 10% lifetime probability of developing breast cancer and a 3% probability of dying from the disease (Grady et al., 1992). The early recognition that breast tumor growth and development was related to estrogen status suggested that compounds that blocked the effect of estrogen, i.e. antiestrogens, may be beneficial in the treatment of related neoplasms (Love, 1991; Spicer and Pike, 1992; Lupu and Lippman, 1993). Tamoxifen is an estrogen antagonist with partial agonist properties which is structurally related to diethylstilbestrol and is currently the treatment of choice for breast cancer in the US (Jordan, 1984; Furr and Jordan, 1984; Buckley and Goa, 1989; Jordan and Murphy, 1990; Jordan, 1994). Adjunctive use of tamoxifen (subsequent to surgical tumor resection) in both pre- and postmenopausal women improves disease-free survival in node-negative breast cancer and increased overall survival in postmenopausal women (Fisher et al., 1989; Fornander et al., 1989; Ziegler and Budzar, 1991; Early Breast Cancer Trialists' Collaborative Group, 1992; Love, 1992; Jaiyesimi et al., 1995). In addition, studies have indicated that tamoxifen decreases the rate of formation of a second primary tumor in the contralateral breast of postoperative patients by approximately 40% (tamoxifen-treated incidence rates, 1.3%; control, 2%) (Love, 1992; Bush and Helzlsouer, 1993; Jaiyesimi et al., 1995). These and other data suggested that tamoxifen may be useful not only in the treatment of breast cancer but also in its prevention. To this end, the National Institutes of Health initiated the Breast Cancer Prevention Trial in 1992, the aim of which was to look at tamoxifen as a prophylactic agent in a large group of women (16 000) at risk for breast cancer (Bush and Helzlsouer, 1993). Tamoxifen has been extensively used (over 4.5 million women/year) and has a relatively benign toxicity profile (Costa, 1993). Nonetheless, the basis for safety changes when a prophylactic, rather than a therapeutic, indication is considered. The major tamoxifen-related side-effects are associated with its hormonal character. Approximately 50% of woman treated with tamoxifen will experience moderate to severe CNS-mediated vasomotor disturbances such as hot flushes and flashes (Love et al., 1991; Jordan, 1992). Other CNS complaints such as depression and cognitive deficits have also been reported and severely affect a subpopulation amounting to between 1 and 5% of users (Nolvadex Adjuvant Trial Organization, 1988; Love, 1992). Recently, however, Cathcart et al. (1993) claims that a much larger population (15%) is affected. These CNS complications are associated with the central antiestrogenic action of the drug.

Based on the poor ability of quaternary salts to penetrate the blood-brain barrier, we have recently designed and synthesized permanently charged tamoxifen analogs, the initial goal of which was to reduce CNS-side effects of tamoxifen (Biegon et al., 1996). The prototype derivative, tamoxifen methiodide (TMI), was found to be largely excluded from the brain. In addition, the compound appeared to be more active than tamoxifen in an in vivo model of human breast cancer and did not stimulate uterine markers for estrogen gene expression (Biegon et al., 1996). TMI was also at least as healthy to bone as estradiol or tamoxifen. The current study was performed to further examine the anti-breast tumor action of TMI using in vivo evaluation with MRI and histological analysis. In addition, mechanism of action was considered by evaluating TMI and tamoxifen in vitro using cultured MCF-7 cells.

2. Materials and methods

2.1. Chemistry

Tamoxifen methiodide was prepared as previously described (Jarman et al., 1986). Briefly, 2.0 g

of tamoxifen (Aldrich, St. Louis, MO) was dissolved in 13 ml of methyl iodide and stirred at 0°C for 24 h. Ethyl acetate was then added to afford a white precipitate, which was recrystallized from methanol to yield tamoxifen methiodide at greater than 99% purity (by HPLC).

2.2. Cell culture studies

Human breast cancer cells (MCF-7 originally obtained from the laboratory of Professor M. Lippman, NIH) were routinely cultured in Dulbeco's Modified Eagle's Medium (DMEM) fortified with 6% fetal calf serum (FCS), penicillin (200 U/ml), streptomycin (200 μg/ml) and neomycin (10 μg/ml) (Furman et al., 1992). For in vitro evaluation, cells were trypsinized from their containers and placed in a DMEM medium without phenol red containing 6% charcoal-stripped fetal calf serum (DCC-FCS). MCF-7 cells (4×10^4/well) were seeded in a 24 well plate. One day later (i.e. at time 0), TMI was added at various concentrations (0.02–20 μM) in a dimethyl sulfoxide (DMSO) vehicle and viable cells, (i.e. those excluding Trypan blue) were counted at days 2, 4, 7 and 9 using a cytometer. The media were changed every two days. In a second set of experiments, cells were prepared as above, but were treated with either estradiol (30 nM), tamoxifen (2 μM), TMI (2 μM) or a combination of either estradiol and tamoxifen or estradiol and TMI at the same concentrations. Cell growth was determined by cell counting at days 2, 4 and 7. For all determinations, analyses were conducted in duplicate with data presented as the average of the two measurements.

2.3. Animal evaluation

Female CD1-nu athymic mice (20–25 g, 6 weeks old) were obtained from the Weizmann Institute Department of Animal Services. MCF-7 cells, serially passed as described above, were detached from the culturing flasks with 0.03% EDTA in phosphate buffered saline (PBS) and washed several times in normal saline (Furman et al., 1992; Degani et al., 1994). Cells (10^7/innoculum) were then injected into the ventral fat pad at the level of the breast. Coincident with cell introduction, a slow-release pellet of estradiol (0.72 mg/pellet, 45 day release profile; Innovative Research, Sarasota, FL) was implanted subcutaneously in the flank of the animal. The pellets contained, in addition to the active ingredient, cholesterol, microcrystalline cellulose, α-lactose, di-and tricalcium phosphate, calcium and magnesium sterate and steric acid and were designed to release estradiol at a constant (zero-order) rate through bioerosion. Mice were anesthetized with ketamine/rompun (i.p.) for the surgical procedures. Within 3–6 weeks, solid tumors were observed in all animals attaining an average size of approximately 1 cm^3. At this point, animals were randomized into three study groups. In the first, animals were sacrificed after imaging and tumors removed for histology (day 0, E2-treated controls, $n = 5$). In the second group ($n = 8$), the estrogen pellet was removed and replaced with a slow-release TMI-laden pellet similar in design to that described above for delivery of estradiol. The pellet contained 6.3 mg of TMI and was prepared to release drug over a 45 day time course. In the third group, the estrogen pellet was removed and replaced with a placebo pellet ($n = 5$). Animals were imaged (under ketamine/rompun anesthesia) either immediately before pellet exchange (day 0) or at day 3, 6, 12 and 25 after pellet exchange. A subgroup of the TMI-treated animals ($n = 4$) were sacrificed at day 3 to allow histological examination. At the conclusion of the experiments, all other animals were sacrificed and tumors collected.

2.4. NMR measurements

MRI images were recorded with a Bruker 4.7 (tesla)/30 Biospec spectrometer (Bruker Medizintechnik, Rheinstetten, Germany). 1H spin-echo images were recorded at 200.12 MHz using a custom-made 4.5 cm rf coil with an image data matrix of 256×128 pixels (Furman et al., 1992; Degani et al., 1994; Furman-Haran et al., 1996). Pilot scans of the tumors were completed using a fast transverse multi-slice spin-echo sequence (giving T1-weighted spectra; inter-echo time (TE) = 16 m/s, recovery time (TR) = 500 m/s) followed by T2-weighted sequences in which axial slices

perpendicular to the spine (i.e. a coronal orientation) were recorded. In the latter case, spin-echo images were obtained using a 4 cm field of view, 1 mm slice thickness, 1.2 mm slice-to-slice distance and a four-sequence average. The TE and TR were optimized to provide the best image contrast generating values of 80 and 3200 m/s, respectively. This gave a total imaging time of approximately 30 min. Under the conditions reported, the in-plane resolution was 155×310 μm. Tumor size was calculated using a slice-to-slice reconstruction in which the slice surface area was obtained from histograms provided by the resident Bruker software package.

For image analysis, the average pixel intensity of viable portions of MCF-7 tumors were determined from a central tumor slice using histograms generated by the dedicated Bruker software package. Necrosis and fibrosis were estimated using pixel by pixel analysis with low intensity necrosis defined as areas demonstrating an increase in intensity of 25–50% over viable areas and high intensity necrosis being associated with areas which were 50% more intense than viable sections. Fibrosis was defined as those area manifesting a decrease in pixel intensity of $\geq 50\%$. Changes in pixel intensity were also examined through the use of standard rainbow color maps. For presentation purposes, all fields of view were normalized to the same maximal intensity.

2.5. Histology

Tumors from estrogen and TMI-treated animals (0–3 days) and from placebo and TMI-treated animals (25 days) were removed after cervical dislocation. Tumors were treated with a biological dye (Davidson Marking Systems, Bradley Products, Bloomington, MN) so that histological sections could be oriented in the same direction as MRI slice images (DeJordy et al., 1992). The histological plane corresponding to the central slice of the MRI study was established by a single cut through the tumor. This plane was based on the position of the tumor in the spectrometer, sagital, transverse and coronal images and anatomical landmarks. The bisected tumors were fixed in 10% formalin, dehydrated in 70% ethanol, blocked in paraffin and 4 μm histological sections cut, placed on slides and stained with either hematoxylin-eosin or a modified trichrome method (DeJordy et al., 1992). Hematoxylin-eosin was used to assess viability, necrosis and pigmentation. The modified trichrome method was applied to the identification of fibrotic regions (i.e. the dye stains for mucopolysaccharides). Sections were examined by a histologist specializing in human breast adenocarcinomas.

3. Results and discussion

Recent studies have demonstrated that quaternization of the anti-breast cancer derivative, tamoxifen (TAM), gives rise to a series of derivatives (e.g. tamoxifen methiodide (TMI)), with several potential pharmacological advantages over the parent agent including (1) decreased CNS penetration, (2) increased specificity of action and (3) increased anticancer action (Biegon et al., 1996). The action of TMI at the level of an implanted human breast tumor was considered herein using MR imaging to permit non-invasive assessment of changes in tumor structure over time after treatment with TMI or placebo.

The model selected involved growing MCF-7 human breast cancer cells in the ventral fat pad (at the level of the breast) of female athymic nude mice (Furman et al., 1991; Furman-Haran et al., 1994). Tumors generated in this way differ in several respects from the standard flank-implanted model including the rapidity with which MCF-7 generate solid masses and growth rate. Flank-implanted tumors generally required 6–10 weeks to achieve a size of 1 cm^3, while MCF-7 cells implanted at the level of the milk line attain these dimensions in 3–6 weeks. Since other difference may also be present, we have revalidated the MRI/histological correlations that have been previously established for the flank-implanted model. Representative tumors sections stained with either hematoxylin-eosin or with a modified trichrome method were selected to provide examples of the histologies of interest. As illustrated in Fig. 1, general tumor contours and geometry were well patterned by the MR images. In this context, the

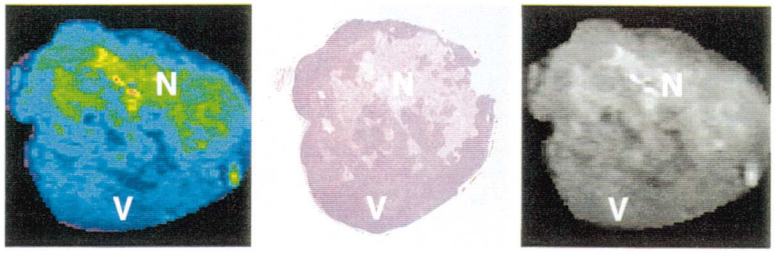

Fig. 1. Comparison of T2-weighted spin-echo images (color-enhanced left, black and white, right) and an hematoxylin-eosin stained histological section (center) of an MCF-7 human breast tumor implanted in a nude mice. 'V' refers to viable tumor areas, while 'N' to necrotic regions. The tumor was treated with TMI for three days after removal of the supportive estradiol pellet.

MRI gives a better representation of in vivo tumor size since the tissue shrinks approximately 20–40% upon fixation and section preparation. Comparisons of the histological sections and MR images indicate that viable tumor areas appeared gray (intermediate intensity) in the T2-weighted spin-echo images, necrotic areas appeared white (hyperintense) due mainly to longer spin-spin relaxation times with some contribution of increased proton density, (i.e. higher water content) and fibrotic areas appeared dark (hypointense) due to shorter spin-spin relaxation times and lower water content. The data are consistent with those generated for the flank-implanted MCF-7 model (Furman et al., 1991, 1992; DeJordy et al., 1992; Degani et al., 1994; Furman-Haran et al., 1994, 1996). With these MR tools for assessing the in vivo tumor viability, the effect of TMI and placebo were assessed on the breast-implanted MCF-7 system. After estrogen-induction and after tumors reached an appropriate size, the supportive estradiol pellet was removed and replaced with either a slow-release (45 day release, 6.3 mg) TMI pellet (s.c.) or a blank (placebo) pellet. Tumors were imaged at high spatial resolution using MRI at day 0 and at days 3, 6, 12 and 25 thereafter. In addition, histological comparisons were made at early time (day 3) and at the end of the experiment (day 25).

Analysis of MR images over time with subsequent reconstruction of tumor slices indicated that TMI induced tumor regression in this study with the MCF-7 neoplasms shrinking an average of 20% over the 25 day time course (Fig. 2). By contrast, animals implanted with a blank pellet manifested continuous tumor growth, which amounted to a 20% increase by the end of the experiment. Placebo-treated tumors grew slower than historical controls in which the estrogen pellet was left in the animals suggesting that pellet removal also exerts a physiological effect consis-

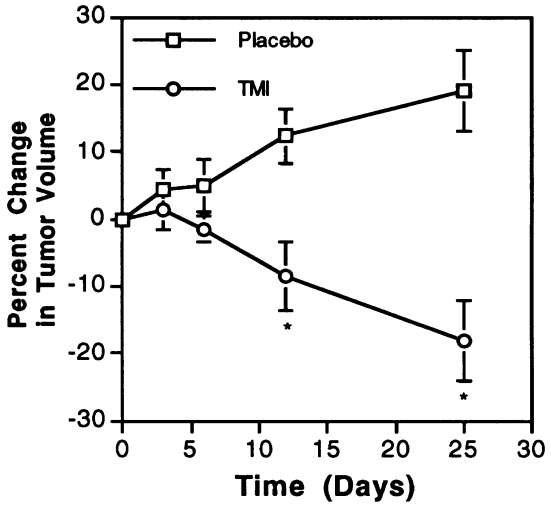

Fig. 2. Effect of TMI and placebo (Partial Estrogen Ablation) on the growth of human breast tumors (MCF-7) implanted into nude mice. Tumor volume was determined by reconstructing of MRI-derived slices (i.e. slice surface area and slice-to-slice distance). * Indicates a significant ($p < 0.05$) reduction in tumor size relative to placebo. Day 25 tumor volumes were significantly larger in the case of placebo and smaller in the case of TMI-treatment, than day 0 values.

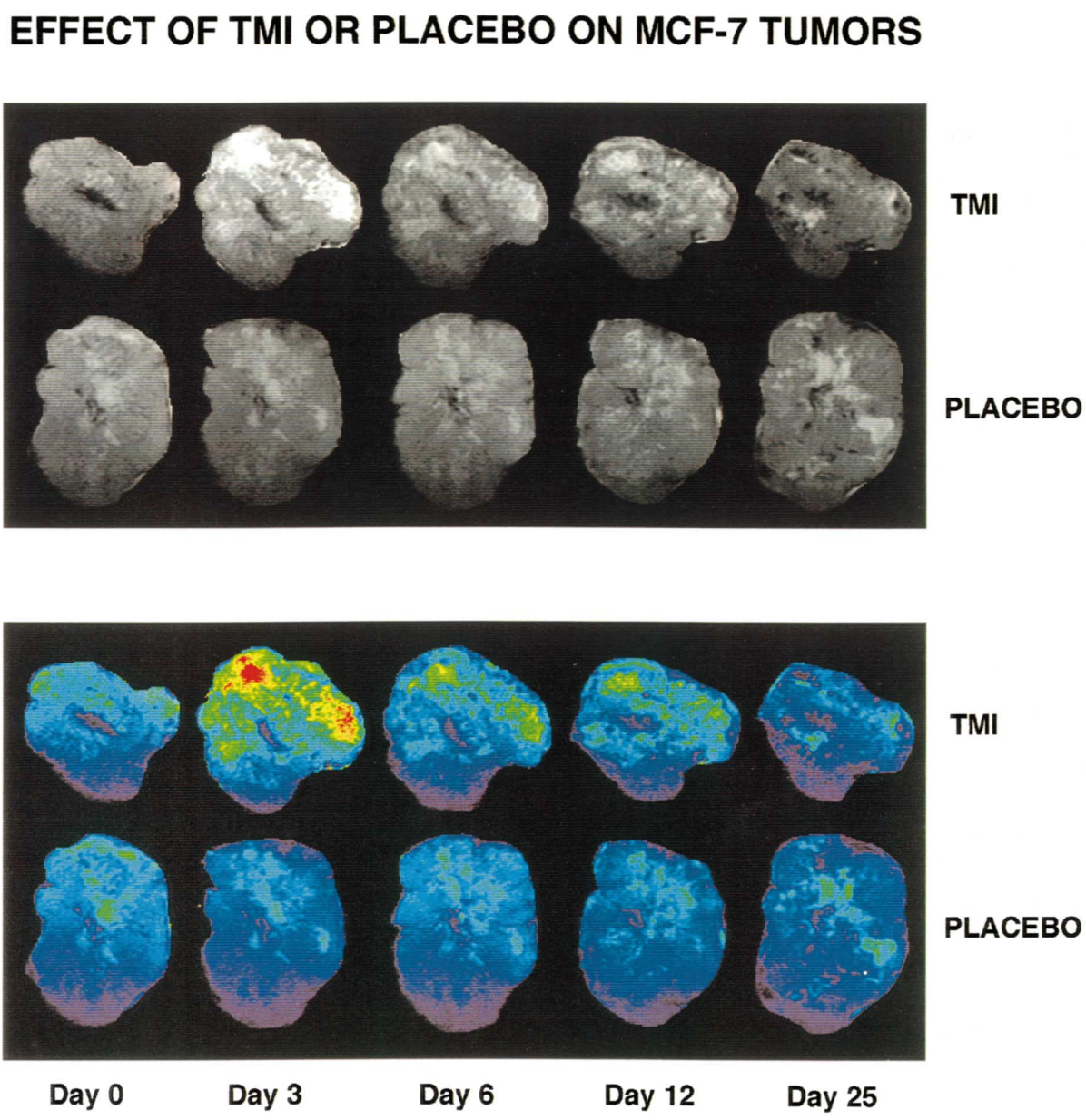

Fig. 3. Effect of TMI or placebo on tumor pathomorphology at various time after initiation of treatment. T2-spin-echo MR images as well as color-enhanced images are presented as described in the Section 2. Necrosis is evident in bright regions of the black and white images (green, yellow or red areas of the pseudocolor images), viable areas are grey in black and white images and blue in the pseudocolor images and fibrosis (showing most prominently at day 25) is black in the black and white T2-images and dark purple in the pseudocolor renderings.

tent with partial hormonal ablation (Furman-Haran et al., 1994). MR images for representative placebo and TMI-treated animals are given in Fig. 3. Two specific parameters were considered in quantitating necrosis: the extent of necrosis (i.e. the portion of the image pixels which manifested

an increase in intensity of 25% above the averaged viable area intensity) as well as the intensity of the necrosis (i.e. to what extent did the pixel intensity increase). Two intensity thresholds were defined including a low intensity necrosis (pixel intensity 25–50% above the average viable area intensity) and high intensity necrosis (pixel intensity $>50\%$ above viable area intensity). According to these definitions, placebo administration did not result in a significant change in tumor necrosis by day 3, but did cause an increase in necrosis by day 6 (Fig. 4). At this time, the area of necrosis was 2-fold higher than that observed on day 0 (increasing from an average of 20% to approximately 40%). Day 0 areas of necrosis were composed mostly of the low intensity subtype (approximately 70% of the total necrotic area) (Fig. 5). At day 6, the proportion of the tumor that was intensely necrotic increased so that it made up about half of the total area of necrosis. Treatment of tumors with TMI provoked a different response in three major respects. First, initiation of tumor-wide necrosis occurred at the first sampling point (day 3) rather than at day 6 as in the case of the placebo. Second, the total area of necrosis increased almost 3-fold from a day 0 average of approximately 25% to a day 3 average

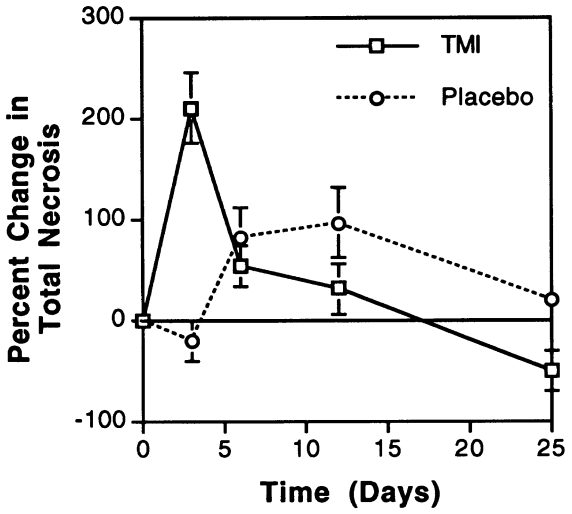

Fig. 4. The percent change in total necrosis relative to day 0 induced by TMI or placebo in MCF-7 human breast tumors implanted in nude mice.

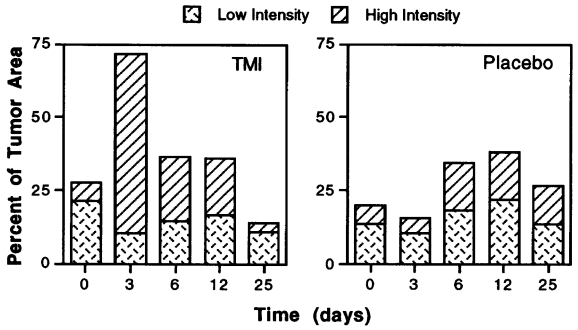

Fig. 5. Effect of TMI (left) and placebo (right) on necrosis in MCF-7 human breast tumors implanted in nude mice. Total necrosis is divided into low and high intensity subtypes and described in the Section 2.

of 72%. Third, the necrosis induced was more intense than that seen in placebo-treated animals with areas of high intensity accounting for 85% of the total necrotic area. All of these initial changes in tumor structure occurred before any significant change in tumor size had become apparent (Furman et al., 1991, 1992; Furman-Haran et al., 1994). In placebo-treated animals, the increase in necrosis, while delayed, was fairly long-lived retreating to baseline levels only by the end of the experiment (day 25). In contrast, TMI-induced necrosis dissipated rapidly but still encompassed about half the tumor by day 12. Interestingly, by the end of the experiment, the areas of necrosis in TMI-treated tumors had generally waned below day 0 data. In both TMI-and placebo-treatments, regression of necrosis was associated with fibrotic infiltration (Fig. 6). In placebo-treated tumors, fibrosis was disseminated through the tumor although the centers of the tumors were generally involved. The same pattern emerged with TMI-treated animals except that areas of fibrosis tended to follow regions of the tumors that had exhibited the most intense necrosis. These histological changes were superimposed on a shrinking TMI-treated but a growing placebo-treated tumor.

Histological analysis of the resected tumors correlated well with the MRI descriptions made above. Day 0 tumors were characterized as well-delimited, moderately differentiated adenocarcinomas. The cytology demonstrated a high

degree of atypia with numerous mitotic figures and prominent nucleoli. While the majority of the day 0 tumors were viable, areas of necrosis were observed which tended to be correlated with tumor size. The reason for this appears to be that as tumors grow, the rapid pace of cell proliferation resulted in compression of the centers of the tumor causing vascular collapse and observed central necrosis (Furman-Haran et al., 1994). In general, the necrosis tends to be a little more extensive in histological sections than in MR images, but this could well be artifactual due to either post-mortem effects or tumor shrinkage as a result of fixation. After 3 days of treatment with TMI, histology revealed that the great majority of the tumor was necrotic, often with viable cells relegated to the tumor margin. At this early time point, fibrosis was not evident. At day 25, the shrinking TMI-treated tumors were composed mostly of necrotic and fibrotic areas (i.e. mostly scar tissue) confirming the MRI assessments.

Thus, TMI induces tumor necrosis that manifests a faster onset, is more extensive and more intense than that induced by partial estrogen ablation (i.e. removal of the estrogen pellet). Furthermore, previous studies indicate that TMI is more potent than tamoxifen in shrinking MCF-7 flank-implanted tumors (Biegon et al., 1996). Preliminary studies also suggest that TMI is more potent than tamoxifen in the breast-implanted model (Y. Paran and H. Degani, unpublished results). Tamoxifen was found to induce rapid necrosis (by day 3) as assessed by MRI but the maximum extent of necrosis was approximately 50% (compared to 72% for TMI) and only about 50% of the necrosis could be characterized as the high intensity subtype (compared to 85% in TMI treated tumors). In addition, while tamoxifen prevented tumor growth, it did not cause a significant reduction in tumor size. There are several explanations for differential anticancer potency of these agents including differences in their interaction with the estrogen receptor or with their cytotoxicity towards breast cancer cells (MCF-7) per se. Two sets of experiments were conducted to explore these possibilities using MCF-7 cells in culture. In the first, the effect of TMI was assayed at various concentrations in the absence of estrogen. Strict exclusion of estrogen required elimination of phenol red from the media (which has weak agonist activity) as well as charcoal stripping of sera (Berthois et al., 1986). As shown in Fig. 7, the effects of TMI on MCF-7 cell growth was highly dose-dependent. At low concentrations (20 and 200 nM), TMI stimulated MCF-7 cell growth relative to the vehicle control, at 2 μM, TMI was cytostatic and at 20 μM, the compound was cytocidal. This pattern of activity is very reminiscent of that seen with tamoxifen. Kawamura et al. (1993), for example, found that tamoxifen stimu-

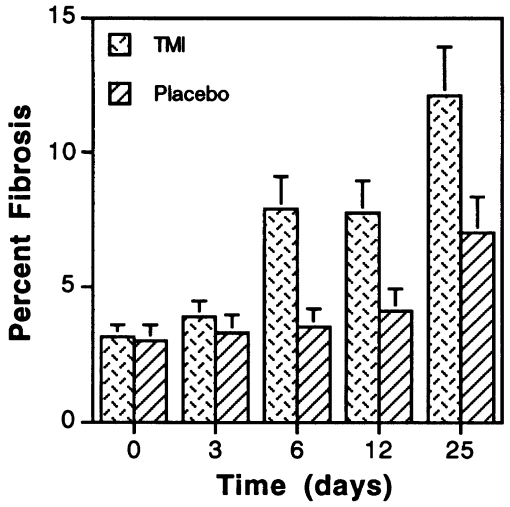

Fig. 6. Effect of TMI or placebo on the development of fibrosis (as defined by MRI) in MCF-7 human breast tumors implanted in nude mice.

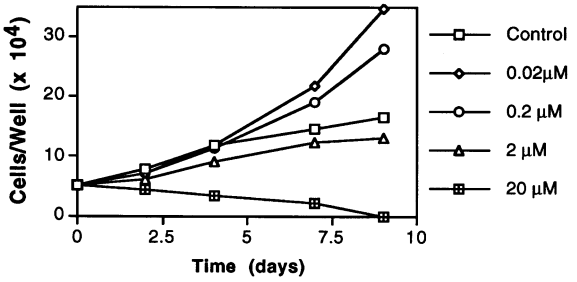

Fig. 7. Effect of TMI at various concentrations on proliferation of MCF-7 cell in cultures. Estrogen was excluded in the study (the media did not contain phenol red and the sera used were stripped with charcoal).

lates the growth of MCF-7 cells in estrogen-free media at concentrations below 10^{-6} M, gives growth kinetics similar to vehicle at 10^{-6} M and was cytotoxic at 10^{-5} M. These data are consistent with the partial agonist properties of tamoxifen, and presumably of TMI, with the estrogenic component being manifested at low doses in an estrogen-free milieu and progressively higher doses manifesting either anti-hormonal action or frank cytotoxicity. The performance of tamoxifen and TMI in the presence of an estrogen was also evaluated (Fig. 8). Again, tamoxifen or TMI at low micromolar concentration (2 μM) is cytostatic. Estradiol (30 nM) stimulates cell proliferation, almost doubling cell number over the time course of the experiment. Co-administration of either TMI or tamoxifen with estrogen, reduces estrogen-stimulated cell growth by 30–50% consistent with previously published reports. For example, tamoxifen, at 1 μM, was shown to reduce estrogen-stimulated cell growth by approximately 30% in a estrogen background of 1 nM (Kawamura et al., 1993). Collectively, these data suggest that TMI and tamoxifen are nearly identical in their interaction with MCF-7 cells, either in the presence or absence of estradiol in keeping with the similar affinity of these agents for the estrogen receptor (with K_i values in the low μM range) (Jarman et al., 1986).

These data suggest that other mechanisms differentially contribute to the anticancer efficacy of

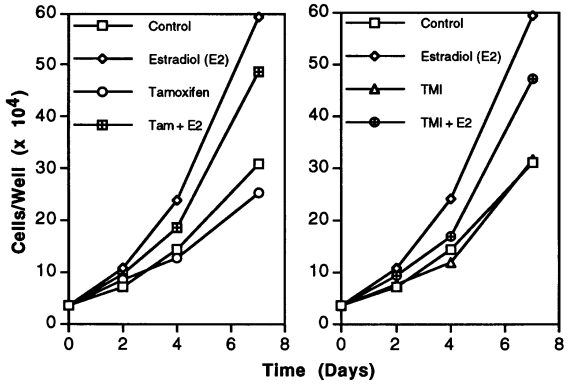

Fig. 8. Effect of tamoxifen (2 μM) (left) and TMI (2 μM) (right) either in the presence (30 nM) or absence of estradiol on the growth of MCF-7 human breast cancer cells in culture.

TMI. Two possibilities in this regard include inhibition of signal transduction and angiogenesis. Cancerous tissue manifests a pathologically rapid rate of cell division which is thought to be related to aberrations in signaling pathways, i.e. alteration in cell mitosis mediated through activation of various phosphorylating enzymes (Levitzki, 1994; Rosen et al., 1995). These enzymes include the protein kinase (i.e. PKC) and phospholipase families (i.e. PLC) (Nishizuka, 1989; Powis and Phil, 1994). Since activation of these enzymes is related to various proliferative diseases, their inhibition may be useful therapeutically. TMI was found to be a more potent inhibitor of both PLC (giving an IC_{50} two to five-fold lower than that associated with tamoxifen (Friedman et al., 1995)) and PKC (giving an IC_{50} ten times lower than that for tamoxifen (Bottega and Epand, 1992)). Finally, there is considerable evidence that cancer growth and dissemination is dependent on angiogenesis (Folkman, 1971, 1990). Therefore, subsequent to the emergence of a tumor, every increase in tumor cell population must be preceded by an increase in capillary density to provide nutrients to the neoplasm. The particular relevance of angiogenesis to human breast cancer has been demonstrated in several experimental paradigms in which both microvessel count and grade correlated with human metastatic disease (Weidner et al., 1991, 1992). In the case of tamoxifen, the speed with which necrosis occurs in implanted breast tumors and the finding that the number of capillaries in the tumor (as indicated by GSL-1 lectin staining) is significantly reduced, has led to the proposition that tamoxifen exerts antiangiogenic action resulting in tumor starvation and the observed cell death (Furman-Haran et al., 1994). Since tamoxifen has been shown to exert these effects both in vitro and in vivo, TMI may demonstrate similar or improved activity as well (Gagliardi and Collins, 1993). Additional factors which may contribute to the differential activity of the two compounds include decreased metabolism of TMI compared to tamoxifen and reduced plasma protein binding of TMI relative to tamoxifen.

MRI is increasingly being used in pharmacological applications in which information on qualita-

tive and quantitative pathomorphology is required (Rudin et al., 1995). This non-invasive technique has been applied in recent years to the evaluation of human breast tumors in both the clinical and experimental setting. Using these methodologies, we have examined the effect of TMI on human breast cancer implanted into the ventral fat pad of female nude mice. The data indicate that TMI induces rapid, extensive and intense necrosis relative to a placebo control. These findings were correlated with, and confirmed by, histological assessments of the treated tumors. In vitro studies indicate that TMI is equal in its potency to tamoxifen, even though TMI appears to be more potent in vivo. The discrepancy between the in vitro and in vivo results may be due to additional mechanism of action exerted by TMI including antiangiogenesis (which cannot be assessed in culture of tumor cells) or inhibition of signal transduction.

Acknowledgements

The authors would like to thanks A. Horwitz for her assistance in reading the histological slides and R. Margalit for aid in completing the animal evaluations. The work was supported by a grant from the National Cancer Institute (CA42238).

References

Berthois, Y., Katzenellenbogen, J., Katzenellenbogen, B., 1986. Phenol red in tissue culture media is a weak estrogen: implications concerning the study of estrogen-responsive cells in culture. Proc. Natl. Acad. Sci. USA 83, 2496–2500.

Biegon, A., Brewster, M., Degani, H., Pop, E., Somjen, D., Kaye, A., 1996. A permanently charged tamoxifen derivative displays anti-cancer activity and improved tissue selectivity in rodents. Cancer Res. 56, 4328–4331.

Bottega, R., Epand, R.M., 1992. Inhibition of protein kinase *C* by cationic amphiphiles. Biochemistry 31, 9025–9030.

Buckley, M., Goa, K., 1989. Tamoxifen, a reappraisal of its pharmacodynamic and pharmacokinetic properties, and therapeutic use. Drugs 37, 451–490.

Bush, T., Helzlsouer, K., 1993. Tamoxifen for the primary prevention of breast cancer: a review and critique of the concept and trial. Epidemiol. Rev. 15, 233–243.

Cathcart, C., Jones, S., Pumroy, C., Peters, G., Knox, S., Cheek, J., 1993. Clinical recognition and management of depression in node negative breast cancer patients treated with tamoxifen. Breast Cancer Res. Treat. 27, 277–281.

Costa, A., 1993. Breast cancer chemoprevention. Eur. J. Cancer 29A, 589–592.

Degani, H., Furman, E., Fields, S., 1994. Magnetic resonance imaging and spectroscopy of MCF-7 human breast cancer: pathophysiology and monitoring of treatment. Clin. Chim. Acta 228, 19–33.

DeJordy, J., Bendel, P., Horwitz, A., Salomon, Y., Degani, H., 1992. Correlation of MR imaging and histologic findings in mouse melanoma. JMRI 2, 695–700.

Early Breast Cancer Trialists' Collaborative Group, 1992. Systemic treatment of early breast cancer by hormonal, cytotoxic or immune therapy. Lancet 339, 1–15 and 71–85.

El-Ashry, D., Lippman, M., 1994. Molecular biology of breast carcinoma. World J. Surg. 18, 12–20.

Fisher, B., Costantino, J., Redmond, C., Poisson, R., Bowman, D., Couture, J., Dimitrov, N., Wolmark, N., Wickerham, D., Fisher, E., Margolese, R., Robidoux, A., Shibata, H., Terz, J., Paterson, A., Feldman, M., Farrar, W., Evans, J., Lickley, H., Ketner., M., 1989. A randomized clinical trial evaluating tamoxifen in the treatment of patients with node-negative breast cancer who have estrogen-receptor positive tumors. N. Engl. J. Med. 320, 479–494.

Folkman, J., 1971. Tumor angiogenesis: therapeutic implications. N. Engl. J. Med. 285, 1182–1186.

Folkman, J., 1990. What is the evidence that tumors are angiogenesis dependent? J. Natl. Cancer Inst. 82, 4–6.

Fornander, T., Cedermark, B., Mattsson, A., Skoog, L., Askergren, J., Rutqvist, L., Glas, U., Silfverswäed, C., Somell, A., Wilking, N. and Hjalmar, M., 1989. Adjuvant tamoxifen in early breast cancer: occurrence of new primary cancers. Lancet I, 117–119.

Friedman, Z., Minz, E., Selinger, Z., 1995. Effects of structural modifications of tamoxifen on phospholipase *C* and phosphoinositide kinase activities. Isr. J. Med. Sci. 31, 758.

Furman, E., Margalit, R., Bendel, P., Horwitz, A., Degani, H., 1991. In vivo studies by magnetic resonance imaging and spectroscopy of the response to tamoxifen of MCF-7 human breast cancer implanted in nude mice. Cancer Commun. 3, 287–297.

Furman, E., Ruskin, E., Margalit, R., Bendel, P., Degani, H., 1992. Tamoxifen induced changes in MCF-7 human breast cancer: in vitro and in vivo studies using nuclear magnetic resonance spectroscopy and imaging. J. Steroid Biochem. Mol. Biol. 43, 189–195.

Furman-Haran, E., Maretzek, A., Goldberg, I., Horwitz, A., Degani, H., 1994. Tamoxifen enhances cell death in implanted MCF-7 breast cancer by inhibiting endothelium growth. Cancer Res. 54, 5511–5514.

Furman-Haran, E., Margalit, R., Grobgeld, D., Degani, H., 1996. Dynamic contrast-enhanced magnetic resonance imaging reveals stress-induced angiogenesis in MCF-7 human breast tumors. Proc. Natl. Acad. Sci. USA 93, 6247–6251.

Furr, B., Jordan, V., 1984. The pharmacology and clinical uses of tamoxifen. Pharmacol. Ther. 25, 127–205.

Gagliardi, A., Collins, D., 1993. Inhibition of angiogenesis by antiestrogens. Cancer Res. 53, 533–535.

Grady, D., Rubin, S., Petitti, D., Fox, C., Black, D., Ettinger, B., Ernster, V., Cummings, S., 1992. Hormone therapy to prevent disease and prolong life in postmenopausal women. Ann. Intern. Med. 117, 1016–1037.

Jaiyesimi, I., Buzdar, A., Decker, D., Hortobagyi G., 1995. Use of tamoxifen for breast cancer: twenty-eight years later. J. Clin. Oncol. 13, 513–529.

Jarman, J., Leung, O., Leclercq, G., Devleeschouwer, N., Stoessel, S., Coombes, C., Skilton, R., 1986. Analogs of tamoxifen: the role of the basic side chain. Application of a whole-cell estrogen-receptor binding assay to *N*-oxide and quaternary salts. Anti-Cancer Drug Des. 1, 259–268.

Jordan, V., 1984. Biochemical pharmacology of antiestrogen action. Pharmacol. Rev. 36, 245–276.

Jordan, V., 1992. Overview from the International Conference on long-term tamoxifen therapy for breast cancer. J. Natl. Cancer Inst. 84, 231–234.

Jordan, V., 1994. Molecular mechanisms of antiestrogen action in breast cancer. Breast Cancer Res. Treat. 31, 41–52.

Jordan, V., Murphy, C., 1990. Endocrine pharmacology of antiestrogens as antitumor agents. Endocrine Rev. 11, 578–610.

Kawamura, I., Mizota, T., Lacey, E., Tanaka, Y., Manda, T., Shimomura, K., Kohsaka, M., 1993. The estrogenic and antiestrogenic activities of droloxifene in human breast cancer. Jpn. J. Pharmacol. 63, 27–34.

Levitzki, A., 1994. Signal-transduction therapy: a novel approach to disease management. Eur. J. Biochem. 266, 1–13.

Love., R., 1991. Antiestrogen chemoprevention of breast cancer: critical issues and research. Prev. Med. 20, 64–78.

Love., R., 1992. Tamoxifen in axillary node-negative breast cancer: multisystem benefits and risks. Cancer Invest. 10, 587–593.

Love., R., Cameron, L., Connell, B., Leventhal, H., 1991. Symptoms associated with tamoxifen treatment in postmenopausal women. Arch. Intern. Med. 151, 1842–1847.

Love., R., Koroltchouk, V., 1993. Tamoxifen therapy in breast cancer control worldwide. Bull. Who 71, 795–803.

Lupu, R., Lippman, M., 1993. The role of erbB2 signal transduction pathways in human breast cancer. Breast Cancer Res. Treat. 27, 83–93.

Nishizuka, Y., 1989. Studies and prospective of the protein kinase *C* family for cellular regulation. Cancer 63, 1892–1903.

Nolvadex Adjuvant Trial Organization, 1988. Controlled trial of tamoxifen as a single adjuvant agent in the management of early breast cancer. Br. J. Cancer 57, 608–611.

Powis, G., Phil, D., 1994. Inhibitors of phosphatidylinositol signaling as antiproliferative agents. Cancer Metast. Rev. 13, 91–103.

Rosen, J., Day, A., Jones, T., Turner, E., Nadzan, A., Stein, R., 1995. Intracellular receptors and signal transducers and activators of transcription superfamilies: novel targets for small-molecule drug discovery. J. Med. Chem. 38, 4855–4874.

Rudin, M., Beckmann, N., Mir, A., Sauter, A., 1995. In vivo magnetic resonance imaging and spectroscopy in pharmacological research: assessment of morphological, physiological and metabolic effects of drugs. Eur. J. Pharm. Sci. 3, 255–264.

Spicer, D., Pike, M., 1992. The prevention of breast cancer through reduced ovarian steroid exposure. Acta Oncol. 31, 167–174.

Telang, N., Bradlow, H., Osborne, M., 1992. Molecular and endocrine biomarkers in non-involved breast: relevance to cancer chemoprevention. J. Cell. Biochem. 16G (Suppl.), 161–169.

Weidner, N., Folkman, J., Pozza, F., Bevilacqua, P., Allred, E., Moore, D., Meli, S., Gasparini, G., 1992. Tumor angiogenesis: a new significant and independent prognostic indicator in early-stage breast carcinoma. J. Natl. Cancer Inst. 84, 1875–1887.

Weidner, N., Semple, J., Welch, W., Folkman, J., 1991. Tumor angiogenesis and metastasis: correlation in invasive breast carcinoma. N. Engl. J. Med. 324, 1–8.

Wong, W., Vijayakumar, S., Weichselbaum, R., 1992. Prognostic indicators in node-negative early stage breast cancer. Am. J. Med. 92, 539–548.

Ziegler, L., Budzar, A., 1991. Current status of adjuvant therapy of early breast cancer. Am. J. Clin. Oncol. 14, 101–110.